Journal of Food and Bioprocess Engineering

Original research

RSM-CFD modeling for optimizing the apricot water evaporation

Azadeh Ranjbar Nedamani*, Seyed Jafar Hashemi

Biosystem Engineering Department, Sari Agricultural Sciences & Natural Resources University, Mazandaran, Iran

ABSTRACT

In this paper, the response surface methodology is complemented with CFD simulation in order to study the optimization of the drying process of apricot slices. A Box-Behnken design was used. The studied factors were velocity of inlet air (A: 0.1-0.9 m/s), the porosity of apricots (B: 0.4- 0.6%), the temperature of inlet air (C: 20-60℃), and the time of drying process (D: 500- 3500 s). Then COMSOL software v. 4.1 was used to simulate the 25 runs derived from RSM design. The results showed the moisture content of samples in lower tray samples (L1-L5) was significantly (p < 0.01) higher than the upper tray samples (U1-U2). The uniformity of inlet air and temperature distribution has a great effect on the final quality of dried samples. Moreover, the inlet air temperature had a significant effect on moisture content. The interaction between the porosity of apricot, the two factors of the inlet air temperature and the drying time had a negative effect on the U-series response. But the best positive interaction effect was due to the air temperature and the drying time. These results show that the final quality is significantly dependent on the drying factors and the uniformity in temperature distribution in the cabinet dryer. The final optimum conditions for apricot drying were 0.6437 for parameter A (Velocity of inlet air), 0.5531 for parameter B (Porosity of apricot), 36.78 for parameter C (temperature of inlet air), and 3233.75 for parameter D (drying time).

Keywords: Drying process; Optimization; RSM technique; CFD simulation; Cabinet dryer

1. Introduction

Drying is an important unit operation in food preservation and helps minimize the postharvest deterioration of perishable foods such as vegetables and fruits. Controlling the drying process parameters is critical during removing water from food material. The final food quality parameters such as color, texture, taste, and final industrial costs of the drying process are affected by selecting an effective combination of process factors. Factors which are related to drying media (such as the humidity, velocity, temperature, sanitation, etc.), food material (such as water content, thickness, size, porosity, composition, sensitivity to possible chemical reactions during drying, heat transfer characteristics, etc.), and drying time can have an important role in food drying (Castro et al., 2018; Chilka & Ranade, 2019).

Drying is a complex process of coupled heat and moisture transfer that should appropriately be understood for different food materials (Chilka & Ranade, 2019). Because of the complexity of food composition, the study and modeling of different foods drying

process is critical (Chilka & Ranade, 2019). One of the most sensitive materials exposed to the drying process is fruits that are highly perishable and drying is a suitable way to stabilize them for further consumptions out of their short shelf-life post-harvesting time (Castro et al., 2018; Chilka & Ranade, 2019). Different methods such as air drying (Curcio & Aversa, 2014; Elmas et al., 2019; Yadollahinia & Jahangiri, 2009), osmotic drying (Azoubel & Murr, 2003; Zecchi & Gerla, 2020), spray drying (Bazaria & Kumar, 2018; Lisboa et al., 2018), and freeze-drying (Gitter et al., 2018; Ishwarya et al., 2015; Moreira et al., 2000) were used to dry the fruit and vegetables. Optimization, modeling, and simulation of the drying process with different types of dryers and processing considerations were reported in the literature (Azmir et al., 2019; Bazaria & Kumar, 2018; Brasiello et al., 2013; Ganesan et al., 2018; Golestani et al., 2013; Sanghi et al., 2017; Sumic et al., 2016; Villegas et al., 2017).

Simulation with computational fluid dynamics (CDF) techniques for fruit drying can be used to study the effect of the different process parameters. Today, CFD modeling and simulation can be helpful to study more detailed process conditions (Chilka &

*Corresponding author.

E-mail address: a.ranjbar@sanru.ac.ir (A. Ranjbar Nedamani).

Ranade, 2019). CFD can be used to calculate the flow behavior of drying media, water removal from food material, and heat transfer analysis during the process (Azmir et al., 2019; Azoubel & Murr, 2003; Sanghi et al., 2017; Villegas et al., 2017). But when we consider multiple process factors during simulations, the application of CFD modeling leads to having a high number of runs that make them hard to analyze. Thus, using a RSM (response surface methodology) technique for reducing the CFD simulation can be helpful to minimize the CFD runs and data analysis time. When a certain response is dependent on several factors, RSM can be used as a collection of statistical and mathematical technique that is used to improve, optimize and develop such processes (Sumic et al., 2016). Because the RSM has the statistical ability to reduce the total treatments in a multi-independent factor study (Misra et al., 2013), it can be a suitable choice before numerical calculations by CFD methods to reduce the final runs behind considering all possible factors including a unit food process.

The aim of this study is the optimization of apricot drying process factors such as inlet air temperature, drying time, inlet air velocity, and apricot porosity. For this reason, an RSM technique was used to find the combination of factors to study their effect. Then a CFD method was used to simulate all combinations for more detailed study. The results from the simulation were used as the final answer in RSM techniques, and then by optimization methods, the final drying model was obtained.

Moreover, a combination of the RSM-CFD method was used to study the effect of process parameters and the characteristics of apricot slices during water removal by laminar airflow in a cabinet dryer. The results can be applied based on the air properties, the position of apricot slices in a cabinet dryer, and the time of the water removing process.

Table 1. The Box-Behnken design.

| Run	Velocity	Porosity	Inlet temperature	Processing time
1	0.5	0.6	40	3500
2	0.5	0.5	40	2000
3	0.5	0.5	20	500
4	0.5	0.6	20	2000
5	0.5	0.5	20	3500
6	0.1	0.5	60	2000
7	0.1	0.5	40	500
8	0.1	0.5	40	3500
9	0.9	0.5	40	500
10	0.1	0.6	40	2000
11	0.5	0.4	40	3500
12	0.9	0.4	40	2000
13	0.5	0.4	20	2000
14	0.9	0.5	40	3500
15	0.5	0.5	60	3500
16	0.5	0.5	60	500
17	0.5	0.6	40	500
18	0.9	0.5	20	2000
19	0.9	0.5	60	2000
20	0.5	0.4	40	500
21	0.1	0.4	40	2000
22	0.5	0.6	60	2000
23	0.5	0.4	60	2000
24	0.1	0.5	20	2000
25	0.9	0.6	40	2000
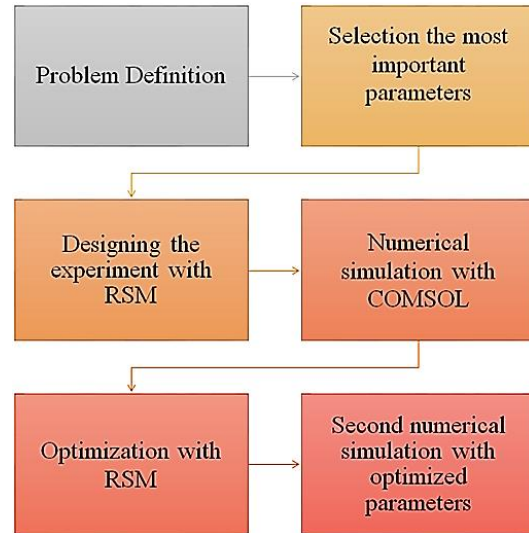
Fig. 1. Research Methodology.

2. Material and Methods

2.1. Experimental Design

The response surface methodology was used to study the effect of important factors of the drying process. A Box-Behnken design with 25 runs was selected by the Design-Expert software version 11 (Table 1). The four factors of the velocity of inlet air (A: 0.1-0.9 m/s), the porosity of apricots (B: 0.4- 0.6%), the temperature of inlet air (C: 20-60℃), and the time of drying process (D: 500- 3500 s) were used. The CFD simulation by COMSOL software was done respectively according to each RSM runs. The final result derived from CFD simulation for each sample (L1- L5, and U1-U5) was moisture content (mol/m^3). After the CFD simulation, the derived results were interred in RSM design and then the responses were analyzed. Finally, a suitable model with statistical significance was selected as a proposed model for apricot drying according to the studied factors (Fig. 1).
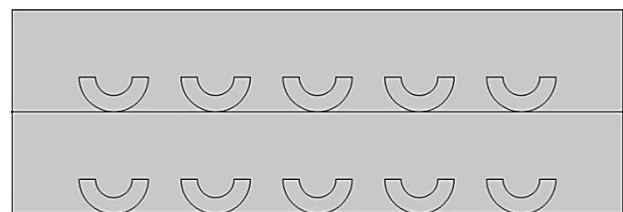
Fig. 2. Geometry meshing (Samples nomenclature from left to right at (1) upper row: U1, U2, U3, U4, and U5; (2) at lower row: L1, L2, L3, L4, and L5).

2.2. Experimental setup

A cabinet drier with 10×30 cm dimensions was considered. The dryer had two stainless steel trays with 5 cm distance from each other. On each tray, 5 apricots with 0.6 cm thickness were placed at 5 cm intervals from each other and the cabinet walls. All apricots were numbered as L1, L2, L3, L4, and L5 for lower tray from left

to the right side and U1, U2, U3, U4, and U5 for upper tray from left to the right side (Fig. 2).

2.3. CFD Model Definition

The basis of this CFD calculation was a laminar airflow through a humid porous medium. The air is dry at the inlet and its moisture content increases as it flows through the porous medium. The flow inside the porous medium is described with the Brinkman equation. The flow in the surrounding domain is from the right side of drier to the left side and is described with the laminar Navier-Stokes equation. The airflow inside each cabinet was assumed based on the work of Darabi et al. 2013. The thermal characteristics of apricot were used based on the work of Cârlescu et al. 2017.

2.4. Governing equations

For a two-dimensional case, the governing equations are as below:

A) Continuity equation
The continuity equation is as Eq. 1:

$$\frac{\partial \rho_a}{\partial \tau} + \nabla(\rho_a . u) = 0 \tag{1}$$

where ρ_a is the density of air (kg/m^3), τ is time (s), ∇ is the del operator, u is Darcian velocity which uses Darcy's Law to calculate the flow field (m/s) (Cârlescu et al., 2017).

B) Momentum equation
The equation for conservation of momentum in an inertial reference frame can be written as follow (Eq. 2) (Cârlescu et al., 2017):

$$\frac{\partial (\rho_a . u)}{\partial \tau} + \nabla(\rho_a . u . u) + \nabla p = 0 \tag{2}$$

where p is the static pressure (Pa).

C) The evaporation of water
In the porous domain, the diffusion coefficient for water vapor into air D_L (m²/s) needs to be adjusted according to Eq. (3):

$$D_e = \frac{\varepsilon_p}{\tau_L} D_L \tag{3}$$

This describes the effective diffusivity inside a porous medium, depending on its structure, characterized by the dimensionless numbers porosity ε_p and tortuosity τ_L. Here, the Bruggeman correction is used, which is according to Eq. (4):

$$D_e = \varepsilon_p^{3/2} D_L \tag{4}$$

Evaporation takes place if the concentration of water vapor is below the equilibrium concentration, which is determined by the saturation concentration c_{sat} and water activity a_w, with Eq. (5):

$$C_{sat} = \frac{P_{sat}(T)}{RT} \tag{5}$$

With the saturation pressure, p_{sat} and the ideal gas constant R = 8.314 J/(mol.K). The water activity describes the amount of water that evaporates into the air. In general, it is a function depending on the water content on a dry basis of the surrounding air and the temperature. Hence the amount of evaporated water is defined as Eq. (6):

$$m_{vap} = K.(a_w c_{sat} - c) \tag{6}$$

where K (1/s) is the evaporation rate, and c the current concentration. The evaporation rate depends on the material properties and the process which causes evaporation. It must be chosen so that the solution is not affected if further increased. This corresponds to assuming that vapor is in equilibrium with the liquid or other words, the time scale for evaporation is much smaller than the smallest time scale of the transport equations. This is true for pore sizes that are not too large. The heat of evaporation is then inserted as a source term in the heat transfer equation according to Eq. (7):

$$Q = H_{vap}.m_{vap} \tag{7}$$

where H_{vap} (J/mol) is the latent heat of evaporation.

2.5. Simulation procedure and geometry modeling

The geometry was meshed using the COMSOL multiphasic software. The mesh consists of 20640 elements. The average element of quality was 0.818. The data from temperature were used to validate the model (Fig. 2). A two-step study was designed; step 1 for stationary modeling of laminar flow module of drying air and step 2 for time dependent modeling of laminar flow, heat transfer in fluids, and transport of diluted species modules. All three modules were coupled with each other through a multiphasic module.

2.6. Statistical analysis

After simulation with CFD method, the moisture content data of each sample (L1-L5, and U1-U5) were collected and statistically analyzed by RSM (Aliakbarian et al., 2018; Atalar & Dervisoglu, 2015). The response variables were fitted to a second-order polynomial model (Eq. 8) which is generally able to describe the relationship between the responses and the independent variables.

$$Y = \beta_0 + \sum_{i=1}^{2} \beta_i X_i + \sum_{i=1}^{2} \beta_{ii} X_i^2 + \sum_{i<i=1}^{2} \beta_{ij} X_{ij} \tag{8}$$

where Y is the response, X_i and X_j are the independent variables affecting the response and β_0, β_i, β_{ii} and β_{ij}, are the regression coefficients for the intercept, linear, quadratic and interaction terms, respectively. To evaluate model adequacy and determine regression coefficients and statistical significance, the analysis of variance (ANOVA) was used. The Design-Expert v.11 was used for RSM statistical analysis. The results were statistically tested at the significance level of $p= 0.01$. The adequacy of the model was evaluated by the coefficient of determination (R^2), model p-value, and lack of fit testing (Aliakbarian et al., 2018; Lisboa et al., 2018; Majeed et al., 2016) and the coefficient of variation (CV). The CV is a measure of deviation from the mean values, which shows the reliability of the experiment. In general, CV<10% indicates better reliability (Islam Shishir et al., 2016). The final optimum parameters proposed by RSM were selected to simulate the optimum conditions with the CFD method. The proposed and the simulated data were compared to study the accuracy of final optimum conditions proposed by RSM.

(a)

(b)
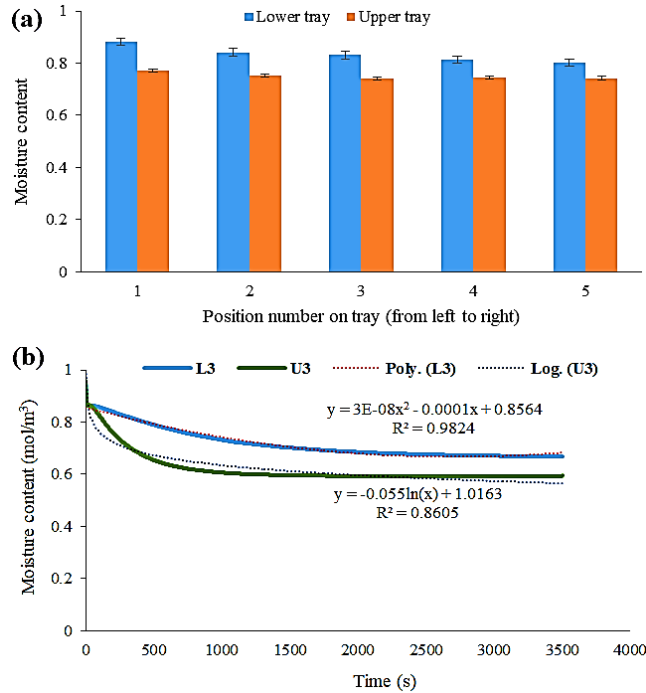
Fig. 3. The changes in moisture content during a complete process time (a) and between samples in two trays (b).

3. Results and Discussion

3.1. Drying Process

Drying was simulated with the CFD method. The parameters such as inlet air velocity, inlet air temperature, the porosity of apricots, and the time of process were considered as model parameters. The RSM technique was used to study the statistical role of each parameter and the further possibility to model the drying process. Data have shown that the mechanism of water evaporation from each sample is different from another (Table 2).

Figs. 3 and 4 show the moisture content in samples. As shown in Fig. 3, the moisture content of samples in lower tray samples (L1-L5) was significantly ($p < 0.01$) higher than the upper tray samples (U1-U2) (Fig. 3a). But the mechanism of drying in two different tray samples is different (Fig. 3b). As can be seen in Fig. 3b, the upper tray samples dry rapidly at the starting times of process, and finally, the rate of drying stops at determined moisture content. But at the lower tray samples, the slope of the graph is different. Eqs. 9 and 10 show the differences in the drying rates of samples according to their place at the trays. As can be seen, the upper tray samples show a logarithmic model with a $R^2 = 0.8605$, while the lower tray samples have a polynomial drying model with $R^2 = 0.9824$.

$$y = 3E - 0.8t^2 - 0.0001t + 0.8564 \quad (R^2 = 0.9824; \text{ Lower tray}) \quad (9)$$

$$y = -0.055\ln(t) + 1.0163 \quad (R^2 = 0.8605; \text{ Upper tray}) \quad (10)$$

Table 2. The Box-Behnken design (BBD) responses for moisture content in 10 samples after simulation with CFD method.

| Run	L1	L2	L3	L4	L5	U1	U2	U3	U4	U5
1	0.881	0.842	0.831	0.814	0.802	0.772	0.753	0.74	0.745	0.743
2	1.07	1.08	1.04	1.01	1	1.02	1	0.97	0.902	0.951
3	1.07	1.08	1.04	1.01	1	1.02	1	0.97	0.902	0.951
4	0.4	0.407	0.408	0.408	0.407	0.358	0.357	0.358	0.361	0.36
5	0.717	0.744	0.747	0.747	0.744	0.544	0.582	0.598	0.61	0.611
6	0.703	0.674	0.667	0.652	0.647	0.616	0.601	0.592	0.596	0.595
7	0.847	0.844	0.841	0.837	0.839	0.733	0.744	0.748	0.751	0.754
8	1.03	0.962	0.956	0.927	0.918	0.888	0.855	0.835	0.843	0.839
9	0.83	0.832	0.826	0.82	0.818	0.698	0.701	0.701	0.701	0.704
10	0.703	0.674	0.667	0.652	0.647	0.616	0.601	0.601	0.596	0.596
11	1.22	1.25	1.18	1.11	1.09	1.05	1.04	1.01	0.989	0.987
12	0.862	0.752	0.746	0.741	0.742	0.713	0.704	0.7	0.7	0.701
13	0.969	0.971	0.951	0.937	0.0928	0.932	0.916	0.887	0.869	0.871
14	0.915	0.916	0.898	0.881	0.875	0.812	0.803	0.883	0.772	0.774
15	0.464	0.442	0.444	0.434	0.434	0.393	0.384	0.379	0.382	0.382
16	1.08	1.09	1.05	1.01	1.01	1.01	0.998	0.972	0.953	0.953
17	1.08	1.09	1.05	1.01	1.01	1.01	0.998	0.972	0.953	0.953
18	0.898	0.887	0.883	0.88	0.881	0.795	0.803	0.804	0.806	0.809
19	0.444	0.443	0.442	0.433	0.435	0.376	0.371	0.369	0.371	0.372
20	0.974	0.966	0.957	0.949	0.944	0.953	0.944	0.938	0.935	0.933
21	0.675	0.661	0.669	0.648	0.655	0.5	0.511	0.503	0.507	0.507
22	0.466	0.472	0.459	0.438	0.437	0.387	0.386	0.378	0.374	0.375
23	0.758	0.752	0.746	0.741	0.742	0.703	0.704	0.7	0.7	0.701
24	0.726	0.75	0.754	0.755	0.755	0.576	0.613	0.62	0.638	0.647
25	0.733	0.728	0.729	0.713	0.716	0.542	0.547	0.543	0.551	0.55
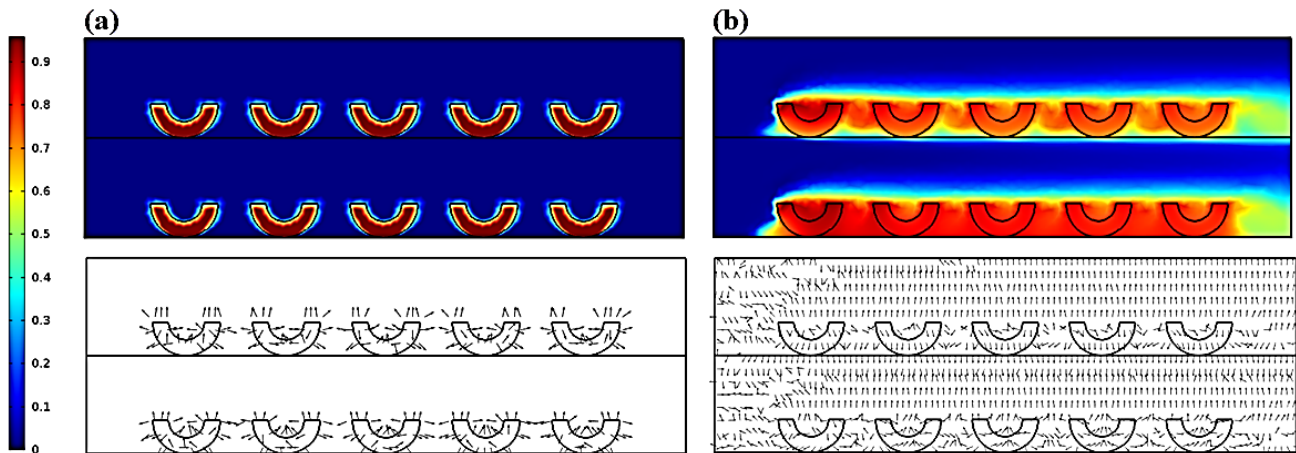
Fig. 4. The moisture content (mol/m^3) and the diffusive flux of water (mol/m^2.s) at the start (a) and the end (b) of drying time.

In both rows of samples, the drying rate will be constant at determined moisture content. But at the upper tray samples, the time of reaching to a constant drying rate is low (1000 s) compared with lower tray samples (2053 s). These two graphs and equations show that the position of samples (Fig. 3b) and the height that the samples are placed for drying in a cabinet dryer (Fig. 4a) can affect the final drying rate and moisture content.

These differences in the moisture content show that the uniformity of inlet air and temperature distribution inside the dryer has a great effect on the final quality of dried food samples (Amanlou & Zomorodian, 2010; Cârlescu et al., 2017; Darabi et al., 2013). Amanlou and Zomorodian (2010) studied the effect of cabinet dryer geometry on the temperature uniformity inside the dryer. They found a new cabinet dryer with a side-mounted plenum chamber that has good uniformity in temperature. Darabi et al. (2013) also designed a new cabinet dryer and studied the effect of different parameters on the final airflow and temperature. They also found that their new design can cover their studied aspects during the drying process.

Fig. 4 shows the schematic distribution of moisture content and diffusive flux of water at the start and the end of the drying process. At the starting time of the process, the moisture content in apricots is high. Also, the water evaporation during the drying process leads to an increase in the moisture content around the apricots and the drying air. But the moisture content inside the apricots decreases.

3.2. Model properties and ANOVA analysis

After simulating all 25 RSM runs with the CFD method, the data for moisture content were analyzed again with RSM. The ANOVA data are presented in Tables 3 and 4 for lower and upper samples, respectively. The adequacy of the model is shown by the coefficient of determination (R^2), model p-value, and lack of fit testing. According to Tables 3 and 4, drying time have a negative relation with the water evaporation rate in L and U series samples. But the inlet air temperature had a significant positive effect on moisture content. The velocity of inlet air and the porosity of apricot had the second and third effective role in the response. The interaction coefficients show the interaction between the porosity of apricot and the two factors of the inlet air temperature and the drying time had a negative effect with U-series response. But the

best positive interaction effect was due to the air temperature and the drying time. In L-series responses, the interaction effects were not significant except the interaction between the inlet air temperature and drying time. These results show that the most effective parameter in drying process was the air temperature. With respect to Eqs. 9 and 10, the final quality is significantly dependent on the uniformity of temperature distribution in the cabinet dryer. This is a positive relation with other literatures (Moghaddam et al., 2017; Villegas et al., 2017; Wani et al., 2017).
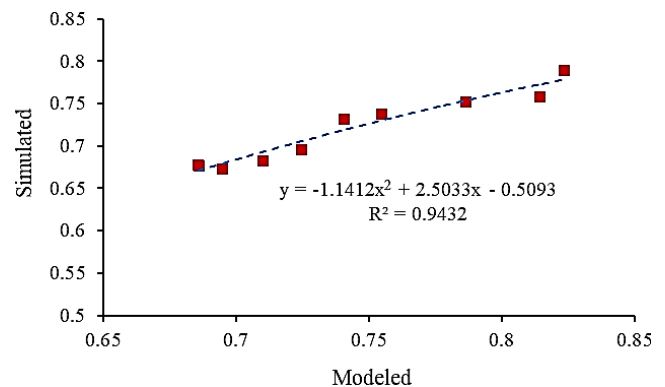
Fig. 5. The comparison between predicted data by RSM model and final examination by CFD.

3.3. Model prediction analysis

According to data analyzed by RSM, the final optimum conditions for apricot drying conditions were 0.6437 for parameter A (Velocity of inlet air), 0.5531 for parameter B (Porosity of apricot), 36.78 for parameter C (temperature of inlet air), and 3233.75 for parameter D (drying time). According to this data, the final optimum model was simulated again by CFD method. The comparison between the predicted data derived from RSM and simulated data is shown in Fig. 5. The correlation was $R^2 = 0.9824$. It shows the combination of a statistical method such as RSM and the numerical simulation method such as CFD can be applicable in simulating-experimental-optimization studies especially when

different factors with different levels need to be studied for one or more qualified responses in food sciences.

Table 3. The ANOVA table of independent process variables on the response and estimated polynomial regression coefficients (L1-L2).

Source	DF	L1 Coefficient	L1 Sum of Squares	L1 p value	L2 Coefficient	L2 Sum of Squares	L2 p value	L3 Coefficient	L3 Sum of Squares	L3 p value	L4 Coefficient	L4 Sum of Squares	L4 p value	L5 Coefficient	L5 Sum of Squares	L5 p value
Model	14	0.9184	1.16	<0.0001	0.8968	1.19	<0.0001	0.8733	1.05	<0.0001	0.8483	0.958	<0.0001	0.75	0.9596	0.0209
Intercept																
Linear																
b1	1	0.0440	0.0303	0.0027	0.0444	0.0308	0.0037	0.037	0.0214	0.0063	0.0254	0.01	0.0411	-0.0178	0.0052	0.6795
b2	1	0.0514	0.0346	0.0017	0.0628	0.0517	0.0006	0.0524	0.036	0.0012	0.0439	0.0253	0.004	0.097	0.1308	0.0524
b3	1	0.2294	0.7292	<0.0001	0.2271	0.7147	<0.0001	0.2136	0.6325	<0.0001	0.2063	0.59	<0.0001	0.159	0.357	0.0035
b4	1	-0.0518	0.0373	0.0013	-0.0596	0.0494	0.0008	-0.0632	0.0555	0.0002	-0.0675	0.0633	0.0002	-0.0109	0.0018	0.8086
Quadratic																
b11	1	-0.1038	0.0403	0.0010	-0.129	0.0623	0.0003	-0.1145	0.049	0.0004	-0.1052	0.0415	0.0008			
b22	1	0.1245	0.0598	0.0002	0.1346	0.0699	0.0002	0.127	0.0622	0.0002	0.1174	0.0531	0.0003			
b33	1	-0.0617	0.0146	0.0201	-0.0283	0.0031	0.2615	-0.0353	0.0048	0.1343	-0.0366	0.0052	0.1235			
b44	1	-0.0921	0.0337	0.0019	-0.0846	0.0284	0.0047	-0.0721	0.0207	0.007	-0.0617	0.0151	0.0165			
Interaction																
b12	1	-0.0079	0.0005	0.6084	0.0089	0.0007	0.5874	0.0023	0	0.8776	-0.002	0	0.8954	0.0427	0.0158	0.4742
b13	1	0.0369	0.0126	0.0284	0.0454	0.0191	0.0143	0.0408	0.0154	0.0154	0.0384	0.0136	0.0212	-0.0154	0.0022	0.7867
b14	1	0.0192	0.0032	0.2230	0.0249	0.0055	0.1431	0.0232	0.0047	0.1368	0.0216	0.0041	0.1638	0.0728		
b23	1	-0.0141	0.0015	0.3947	-0.0187	0.0027	0.2919	-0.0206	0.0033	0.2094	-0.0224	0.0039	0.1761	0.0337		
b24	1	-0.0011	8.71E-06	0.9476	0.0018	0	0.9194	-0.0037	0.0001	0.8192	-0.0065	0.0003	0.6884	-0.0577		
b34	1	0.1427	0.1625	<0.0001	0.1364	0.1485	<0.0001	0.1343	0.144	<0.0001	0.1275	0.1297	<0.0001			
Residual	10		0.0192			0.0218			0.0181			0.0183				
Lack of fit	5		0.0105	0.4255		0.0164	0.1246		0.0133	0.1449		0.0147	0.0723			
Pure error	5		0.0088			0.0054			0.0048			0.0036				
Total	24		1.18			1.22			1.07			0.9763				
R²		0.9837			0.9821			0.9831			0.9813			0.7018		
Adj-R²		0.9609			0.9571			0.9594			0.9550			0.4888		
CV		5.34			5.74			5.32			5.47			22.89		

Indices 1, 2, 3, and 4 refer to velocity of inlet air, porosity of apricot, inlet air temperature, drying time, respectively. The 11 illustrates the interaction effect between factor 1 and 1 and so on. The 12 illustrates the interaction effect between factors 1 and 2 and so on.

Table 4. The ANOVA table of independent process variables on the response and estimated polynomial regression coefficients (U1-U2).

Source	DF	U1 Coefficient	U1 Sum of Squares	U1 P value	U2 Coefficient	U2 Sum of Squares	U2 P value	U3 Coefficient	U3 Sum of Squares	U3 P value	U4 Coefficient	U4 Sum of Squares	U4 P value	U5 Coefficient	U5 Sum of Squares	U5 P value
Model	14	0.8253	1.19	<0.0001	0.8082	1.11	<0.0001	0.7913	1.04	<0.0001	0.7646	0.9126	<0.0001	0.7807	0.9526	<0.0001
Intercept																
Linear																
b1	1	0.0323	0.0163	0.0482	0.0251	0.0098	0.1225	0.025	0.0098	0.1616	0.0127	0.0025	0.3781	0.011	0.0019	0.448
b2	1	0.0449	0.0264	0.0169	0.0474	0.0294	0.0153	0.0471	0.0291	0.0261	0.0412	0.0223	0.0205	0.0389	0.0199	0.0288
b3	1	0.2393	0.7938	<0.0001	0.2304	0.7361	<0.0001	0.2239	0.6948	<0.0001	0.2079	0.5989	<0.0001	0.2141	0.6353	<0.0001
b4	1	-0.0352	0.0172	0.0437	-0.0437	0.0265	0.0198	-0.0514	0.0368	0.0151	-0.0433	0.026	0.014	-0.0463	0.0298	0.0108
Quadratic																
b11	1	-0.132	0.0652	0.0012	-0.1263	0.0597	0.002	-0.1049	0.0412	0.0112	-0.0941	0.0331	0.0073	-0.1092	0.0446	0.0033
b22	1	0.1412	0.0769	0.0006	0.138	0.0734	0.001	0.1245	0.0598	0.0039	0.1398	0.0754	0.0005	0.1279	0.0631	0.0011
b33	1	-0.0343	0.0045	0.2634	-0.0285	0.0031	0.3642	-0.0434	0.0072	0.2228	-0.0561	0.0121	0.0698	-0.0357	0.0049	0.2336
b44	1	-0.1124	0.0501	0.0028	-0.1022	0.0415	0.0061	-0.0813	0.0262	0.0329	-0.0709	0.0199	0.0264	-0.0827	0.0271	0.0138
Interaction																
b12	1	0.0071	0.0004	0.7235	0.0096	0.0008	0.6441	0.0172	0.0025	0.459	0.0025	0.0001	0.8959	0.0044	0.0002	0.8222
b13	1	0.0358	0.0119	0.084	0.0353	0.0115	0.0977	0.0413	0.0158	0.0837	0.0307	0.0087	0.1162	0.0317	0.0093	0.1111
b14	1	0.0042	0.0002	0.8325	0.0106	0.001	0.6042	0.0033	0.0001	0.8836	0.0171	0.0026	0.3716	0.0184	0.003	0.3445
b23	1	-0.0328	0.0083	0.1404	-0.0342	0.009	0.1379	-0.0255	0.005	0.3052	-0.0333	0.0085	0.1198	-0.0337	0.0087	0.1218
b24	1	-0.0105	0.0008	0.6266	-0.0095	0.0007	0.6704	-0.0207	0.0032	0.4105	-0.0149	0.0016	0.474	-0.0125	0.0011	0.5544
b34	1	0.0983	0.0772	0.0006	0.1016	0.0825	0.0006	0.0926	0.0685	0.0025	0.1065	0.0906	0.0002	0.1036	0.0858	0.0003
Residual	10		0.0323			0.0345			0.0429			0.0295			0.0305	
Lack of fit	5		0.0295	0.0108		0.0329	0.0024		0.0417	0.0006		0.0281	0.0023		0.0293	0.0015
Pure error	5		0.0028			0.0016			0.0011			0.0014			0.0012	
Total	24		1.22			1.15			1.08			0.942			0.9831	
R²		0.9736			0.9699			0.9603						0.9690		
Adj-R²		0.9367			0.9278			0.9048						0.9256		
CV		7.88			8.20			9.21						7.84		

Indices 1, 2, 3, and 4 refer to velocity of inlet air, porosity of apricot, inlet air temperature, drying time, respectively. The 11 illustrates the interaction effect between factor 1 and 1 and so on. The 12 illustrates the interaction effect between factors 1 and 2 and so on.

4. Conclusion

Since the cabinet dryers are simple in structure and have low-cost illustration, they can be used readily in fruit drying processes. Today with CFD simulation, it can be possible to study the effect of different parameters in food drying, and thus, different factors can be considered in illustrating a dryer. But CFD simulations with different undertaken parameters make it difficult and time-consuming to study the exact effect of parameters during drying. Herewith the help of the RSM technique, it is possible to statistically study the different parameters and their considered range in CFD simulations. This study showed the combination of these two effective methodologies is a good practice to study the CFD simulations in processes with multiple parameters in different ranges. The results show that the final quality is significantly dependent on the drying factors and the uniformity in temperature distribution in the cabinet dryer.

Acknowledgment

Conflict of interest

The authors declare that they have no known competing financial interests or personal relationships that could have appeared to influence the work reported in this paper.

References

Aliakbarian, B., Sampaio, F. C., de Faria, J. T., Pitangui, C. G., Lovaglio, F., Casazza, A. A., … Perego, P. (2018). Optimization of spray drying microencapsulation of olive pomace polyphenols using Response Surface Methodology and Artificial Neural Network. *LWT*, *93*, 220-228.

Amanlou, Y., & Zomorodian, A. (2010). Applying CFD for designing a new fruit cabinet dryer. *Journal of Food Engineering*, *101*(1), 8-15.

Atalar, I., & Dervisoglu, M. (2015). Optimization of spray drying process parameters for kefir powder using response surface methodology. *LWT - Food Science and Technology*, *60*(2, Part 1), 751-757.

Azmir, J., Hou, Q., & Yu, A. (2019). CFD-DEM simulation of drying of food grains with particle shrinkage. *Powder Technology*, *343*, 792-802.

Azoubel, P. M., & Murr, F. E. X. (2003). Optimisation of osmotic dehydration of cashew apple (*Anacardium occidentale* L.) in sugar solutions. *Food Science and Technology International*, *9*(6), 427-433.

Bazaria, B., & Kumar, P. (2018). Optimization of spray drying parameters for beetroot juice powder using response surface methodology (RSM). *Journal of the Saudi Society of Agricultural Sciences*, *17*(4), 408-415.

Brasiello, A., Adiletta, G., Russo, P., Crescitelli, S., Albanese, D., & Di Matteo, M. (2013). Mathematical modeling of eggplant drying: Shrinkage effect. *Journal of Food Engineering*, *114*(1), 99-105.

Cârlescu, P.-M., Arsenoaia, V., Roşca, R., & ţenu, I. (2017). CFD simulation of heat and mass transfer during apricots drying. *LWT - Food Science and Technology*, *85*, 479-486.

Castro, A. M., Mayorga, E. Y., & Moreno, F. L. (2018). Mathematical modelling of convective drying of fruits: A review. *Journal of Food Engineering*, *223*, 152-167.

Chilka, A. G., & Ranade, V. V. (2019). CFD modelling of almond drying in a tray dryer. *The Canadian Journal of Chemical Engineering*, *97*(2), 560-572.

Curcio, S., & Aversa, M. (2014). Influence of shrinkage on convective drying of fresh vegetables: A theoretical model. *Journal of Food Engineering*, *123*, 36-49.

Darabi, H., Zomorodian, A., Akbari, M. H., & Lorestani, A. N. (2013). Design a cabinet dryer with two geometric configurations using CFD. *Journal of Food Science and Technology*, *52*(1), 359-366.

Elmas, F., Varhan, E., & Koç, M. (2019). Drying characteristics of jujube (*Zizyphus jujuba*) slices in a hot air dryer and physicochemical properties of jujube powder. *Journal of Food Measurement and Characterization*, *13*(1), 70-86.

Ganesan, V., Gurumani, V., Kunjiappan, S., Panneerselvam, T., Somasundaram, B., Kannan, S., … Bhattacharjee, C. (2018). Optimization and analysis of microwave-assisted extraction of bioactive compounds from *Mimosa pudica* L. using RSM & ANFIS modeling. *Journal of Food Measurement and Characterization*, *12*(1), 228-242.

Gitter, J. H., Geidobler, R., Presser, I., & Winter, G. (2018). Significant drying time reduction using microwave-assisted freeze-drying for a monoclonal antibody. *Journal of Pharmaceutical Sciences*, *107*(10), 2538-2543.

Golestani, R., Raisi, A., & Aroujalian, A. (2013). Mathematical modeling on air drying of apples considering shrinkage and variable diffusion coefficient. *Drying Technology*, *31*(1), 40-51.

Ishwarya, S. P., Anandharamakrishnan, C., & Stapley, A. G. F. (2015). Spray-freeze-drying: A novel process for the drying of foods and bioproducts. *Trends in Food Science & Technology*, *41*(2), 161-181.

Islam Shishir, M. R., Taip, F. S., Aziz, N. A., Talib, R. A., & Hossain Sarker, M. S. (2016). Optimization of spray drying parameters for pink guava powder using RSM. *Food Science and Biotechnology*, *25*(2), 461-468.

Lisboa, H. M., Duarte, M. E., & Cavalcanti-Mata, M. E. (2018). Modeling of food drying processes in industrial spray dryers. *Food and Bioproducts Processing*, *107*, 49-60.

Majeed, M., Hussain, A. I., Chatha, S. A., Khosa, M. K., Kamal, G. M., Kamal, M. A., … Liu, M. (2016). Optimization protocol for the extraction of antioxidant components from *Origanum vulgare* leaves using response surface methodology. *Saudi Journal of Biological Sciences*, *23*(3), 389-396.

Misra, S., Raghuwanshi, S., & Saxena, R. K. (2013). Statistical approach to study the interactive effects of process parameters for enhanced xylitol production by *Candida tropicalis* and its potential for the synthesis of xylitol monoesters. *Food Science and Technology International*, *19*(6), 535-548.

Moghaddam, A. D., Pero, M., & Askari, G. R. (2017). Optimizing spray drying conditions of sour cherry juice based on physicochemical properties, using response surface methodology (RSM). *Journal of Food Science and Technology*, *54*(1), 174-184.

Moreira, R., Figueiredo, A., & Sereno, A. (2000). Shrinkage of apple disks during drying by warm air convection and freeze drying. *Drying Technology*, *18*(1-2), 279-294.

Sanghi, A., Ambrose, R. P. K., & Maier, D. (2017). CFD simulation of corn drying in a natural convection solar dryer. *Drying Technology*, *36*(7), 859-870.

Sumic, Z., Vakula, A., Tepic, A., Cakarevic, J., Vitas, J., & Pavlic, B. (2016). Modeling and optimization of red currants vacuum drying process by response surface methodology (RSM). *Food Chemistry*, *203*, 465-475.

Villegas, J. F., Cruz, H. S. D. L., Altamar, F. B., Lozano, W. O., & Silvera, A. B. (2017). Obtaining fruit-drying curves and CFD analysis for corozo (*Bactris guineensis*). *Contemporary Engineering Sciences*, *10*, 569-577.

Villegas, J. F., De La Cruz, H. S., Altamar, F. B., & Lozano, W. O. (2017). CFD numeric simulation to obtain the proper parameters of corozo drying (*Bactris guineensis*). *Contemporary Engineering Sciences*, *10*, 703-711.

Wani, S. M., Jan, N., Wani, T. A., Ahmad, M., Masoodi, F. A., & Gani, A. (2017). Optimization of antioxidant activity and total polyphenols of dried apricot fruit extracts (*Prunus armeniaca* L.) using response surface methodology. *Journal of the Saudi Society of Agricultural Sciences*, *16*(2), 119-126.

Yadollahinia, A., & Jahangiri, M. (2009). Shrinkage of potato slice during drying. *Journal of Food Engineering*, *94*(1), 52-58.

Zecchi, B., & Gerla, P. (2020). Effective diffusion coefficients and mass flux ratio during osmotic dehydration considering real shape and shrinkage. *Journal of Food Engineering*, *274*, 109821.